Linking the disease transmission to information dissemination dynamics: An insight from a multi-scale model study

Tangjuan Li, Yanni Xiao *

School of Mathematics and Statistics Xi'an Jiaotong University, Xi'an 710049, PR China

ABSTRACT

During the outbreak of emerging infectious diseases, information dissemination dynamics significantly affects the individuals' psychological and behavioral changes, and consequently influences on the disease transmission. To investigate the interaction of disease transmission and information dissemination dynamics, we proposed a multi-scale model which explicitly models both the disease transmission with saturated recovery rate and information transmission to evaluate the effect of information transmission on dynamic behaviors. Considering time variation between information dissemination, epidemiological and demographic processes, we obtained a slow-fast system by reasonably introducing a sufficiently small quantity. We carefully examined the dynamics of proposed system, including existence and stability of possible equilibria and existence of backward bifurcation, by using the fast-slow theory and directly investigating the full system. We then compared the dynamics of the proposed system and the essential thresholds based on two methods, and obtained the similarity between the basic dynamical behaviors of the slow system and that of the full system. Finally, we parameterized the proposed model on the basis of the COVID-19 case data in mainland China and data related to news items, and estimated the basic reproduction number to be 3.25. Numerical analysis suggested that information transmission about COVID-19 pandemic caused by media coverage can reduce the peak size, which mitigates the transmission dynamics during the early stage of the COVID-19 pandemic.

© 2021 Elsevier Ltd. All rights reserved.

1. Introduction

Emerging infectious diseases, including SARS(2003),H1N1(2009) and COVID-19, have always been a threat to human healths, bringing a great disaster to human survival and economic development (Crossley et al., 2020; Khardori, 2009; Smith, 2006; COV, 2020; Thompson et al., 2003). In the era of information development, the spread of infectious diseases has been accompanied by the rapid spread of information (globally/locally available information). On the one hand, the disease-related information, can make people more understand the infectious diseases, including the transmission routes, infectivity and possible prevention and control measures, so as for individuals to take effective protective measures. On the other hand, it may also cause panic and bring some social problems (Jansen et al., 2003). Therefore, the dissemination disease-related information consequently induce individuals' behavioural changes, which greatly affects disease transmission (Schaller, 2011; Funk et al., 2010b; Frederik et al., 2016).

A number of ordinary differential equation models are used to analyze the impact of individuals' behaviour changes, such as wearing face masks, keeping social distancing, etc, in response to the dissemination disease-related information. Basically, there are two types of studies considering the transmission of the disease-related information: One is to hypothesize that behavioral changes lead to a reduction in infection rate or contact rate, such as modeling the infection rate as a function of the number of infected individuals (Cui et al., 2008b; Song and Xiao, 2017; Wang and Xiao, 2014; Xiao et al., 2015; Xiao et al., 2013; Zhang et al., 2004; Zhou et al., 2019) or number of news items (Yan et al., 2016; Song et al., 2019), where news items are considered as a separate compartment. In particular, the reduction in infection rate may be determined by the payoff gains using game theory (imitation dynamics) (Frank, 2020; Reluga and Bergstrom, 2010), and the reduction in contact rate may be induced by government shutdown policies as well as individuals' adherence to non-pharmaceutical intervention (Pcja et al., 2021). The other is to further divide the population into two types of compartments with or without disease-related information (Amaral et al., 2021; Shannon et al., 2015; Funk et al., 2010a; Samanta and Chattopadhyay, 2014;

Samanta et al., 2013; Zhao et al., 2020), and those who knowing information may subconsciously protect themselves from the disease and consequently reduce the contact rates or transmission probability. Note that the shift between the disease-aware group and disease-unaware group was modelled and determined by the payoff gains for changing behaviors or not (Amaral et al., 2021; Zhao et al., 2020). The second modelling approach actually provides a scheme of the explicit modelling the transmission of information, which inevitably increases the dimension of the system and brings much difficulties in theoretical analysis. How to nest the dynamics of information transmission dynamics to the disease transmission, and theoretically analyze the dynamical behavior remain unclear and fall with in the scope of this study.

The COVID-19 pandemic has been threatening the public health and caused worrying concern amongst the public and health authorities (Cohen and Normile, 2020; Crossley et al., 2020; Winskill et al., 2020; COV, 2020). As early as the beginning of 2020 when the outbreak of COVID-19 infection was reported in Wuhan, China, massive news coverage and fast information flow significantly generated profound psychological/behavioural impacts on the public, which may influence the implementation of public interventions (Shannon et al., 2015; Xiao et al., 2015; Zhou et al., 2020). Actually, Wise et al. (2020) has testified the importance of risk perception in early interventions during large-scale pandemic. Many researchers (Amaral et al., 2021; Frank, 2020; Pcja et al., 2021; Zhao et al., 2020) also analyzed the impact of behavioral changes induced by disease-related information on COVID-19 transmission from different aspects, which all show that behavioral changes have potential to curb the transmission of COVID-19 infection. Further, Amaral et al. (2021) and Frank (2020) showed the occurrence of multiple outbreaks, which is the synergy between infection prevalence and prevalence-induced interventions and behaviour changes. These models suppose that the spread of the epidemic and transmission of information occurs at the same time scale. However, the dissemination of information among individuals is fast compared to the disease spread. Considering the very differential time scales between information dissemination and disease spread through a mathematical modeling framework falls within another scope of this study.

Main purpose of this study is to propose the multi-scale model which explicitly models both the disease transmission with saturated recovery rate and information transmission, and further divide different classes based on epidemiological characteristics into two subclasses with different infection rates. Considering the very time scales between information dissemination and epidemiological and demographic processes, we introduced a sufficiently small quantity which is determined by population death rate and media wading rate, on this basis, the dynamical behaviour of the proposed model was analyzed using the theory of the slow-fast system (Cen et al., 2014; Feng et al., 2013; Feng et al., 2015). Moreover, the similarity between the basic dynamical behaviors of the slow system and that of the full system is confirmed through theoretical and numerical analyses. Finally, we parameterized the proposed model on the basis of the COVID-19 confirmed cases data in mainland China and data on news items at early period of COVID-19 infection, and estimated the transmission risk. The influence of information transmission about disease caused by media coverage on the peak size of the infection during the early stage of the COVID-19 outbreak was further investigated. We emphasize that this model is not an empirical description of the current COVID-19 evolution. Instead, this is a general theoretical framework that merges disease transmission and information dissemination in a single compartmental model and take into account of time variation between information dissemination, epidemiological and demographic process.

2. The model

We take a classic SIR-type model to illustrate how to model disease and information transmission. For this purpose, we divide the population into susceptible individuals (S), infectious individuals (I) and removed individuals (R). Taking into account the transmission of information and the individual's response to the information acquired, the population is further divided into two groups: one group is disease-unaware group (S_1, I_1, R_1), the other is disease-aware group (S_2, I_2, R_2) who get information about the disease and make behavioral changes to reduce their contacts or improve protection interventions. We assume that the susceptible individuals are infected by infectious individuals with a rate of β, and become infectious, and the infected individuals are recovered with a saturated function $\frac{\gamma}{1+hI_i}, (i = 1, 2)$ given the limitation of medical resources (Zhou and Cui, 2011; Xu and Liu, 2008; Cui et al., 2008a; Jinliang et al., 2012).

Let the variable B be the average number of news items related to the outbreak, with which the disease-unaware individuals will become the disease-aware individuals at the rate α, where α represents the probability of an individual making behavior changes after receiving disease-related information, and parameter β, the transmission probability that a susceptible individual becomes infected after contacting with an infected individual. The disease-aware individuals can also change to the disease-unaware individuals with rate of q. It is assumed that the changing rate of the average number of daily news items depends on the number of infected individuals with rate of ρ, and parameter d represents the spontaneous disappearance rate of media reports(media wading rate). The model flow diagram is shown in Fig. 1 and the model equations are as follows.

$$
\begin{cases}
\frac{dS_1}{dt} = \mu - \beta S_1 I_1 - \sigma_I \beta S_1 I_2 - \mu S_1 - \alpha B S_1 + q S_2 \\
\frac{dS_2}{dt} = -\sigma_S \beta S_2 I_1 - \sigma_I \sigma_S \beta S_2 I_2 - \mu S_2 + \alpha B S_1 - q S_2 \\
\frac{dI_1}{dt} = \beta S_1 I_1 + \sigma_I \beta S_1 I_2 - \frac{\gamma I_1}{1+hI_1} - \mu I_1 - \alpha B I_1 + q I_2 \\
\frac{dI_2}{dt} = \sigma_S \beta S_2 I_1 + \sigma_S \sigma_I \beta S_2 I_2 - \frac{\gamma I_2}{1+hI_2} - \mu I_2 + \alpha B I_1 - q I_2 \\
\frac{dR_1}{dt} = \frac{\gamma I_1}{1+hI_1} - \mu R_1 - \alpha B R_1 + q R_2 \\
\frac{dR_2}{dt} = \frac{\gamma I_2}{1+hI_2} - \mu R_2 + \alpha B R_1 - q R_2 \\
\frac{dB}{dt} = \rho(I_1 + \theta I_2) - dB
\end{cases}
\tag{2.1}
$$

Here we assume that the birth balances the death with the rate of μ, and mortality due to disease is not considered. Therefore, S_j, I_j, and $R_j, j = 1, 2$ can be considered as the corresponding population proportion. Parameters σ_I and σ_S ($0 < \sigma_I, \sigma_S < 1$) represent the reduction factors in transmission rate when infection occurs between disease-unaware group and disease-aware group. In particular, when a susceptible individual (S_2) is infected by an infected individual (I_2), then the reduction factor becomes $\sigma_I \sigma_S$. Parameter θ represent the adjustment factor of the changing rate of the average number of daily news item depends on the number of aware infected individuals.

It is obvious that the solution of system (2.1) initiating from the non-negative data are non-negative.

3. Dynamical analysis

3.1. Establishment of slow-fast system

We know that awareness spreads much faster than population growth. That is, the parameters in model (2.1) have different time scales. So we can use the theory of the slow-fast system to analyze this model. We then reasonably assume that the birth (or death)
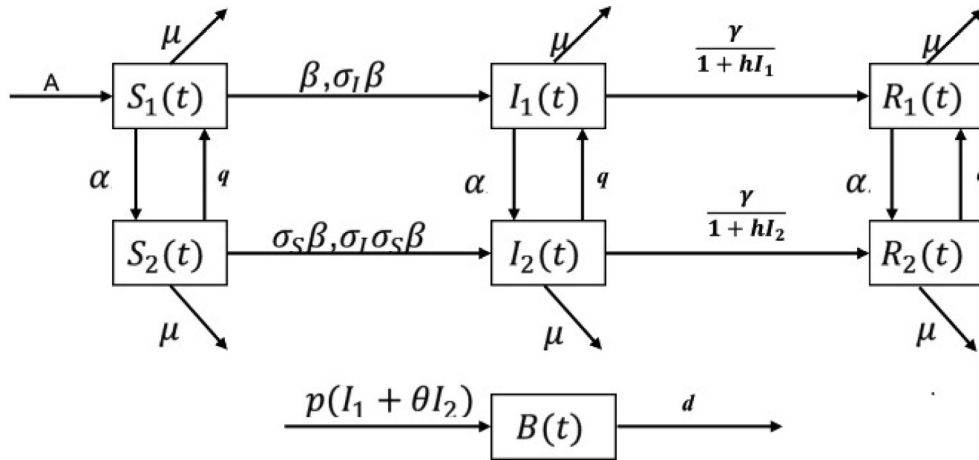
Fig. 1. Flow diagram for a SIRB model that links the disease transmission to information transmission.

rate of population, μ, is much less than the infection wading rate d. To reduce the number of parameters, we assume $\theta = 1$. Making $\varepsilon = \frac{\mu}{d}$, then $0 < \varepsilon \ll 1$. Let

$$\tilde{t} = \mu t, \tilde{\alpha} = \frac{\alpha}{d}, \tilde{\rho} = \frac{\rho}{d}, \tilde{q} = \frac{q}{d}, \tilde{\gamma} = \frac{\gamma}{\mu}, \tilde{\beta} = \frac{\beta}{\mu}, \tag{3.2}$$

and for the sake of simplicity, the parameters of subsequent models are still recorded as the original parameters, then the system on the slow time scale (3.3) is established:

$$\begin{cases} \varepsilon \frac{dS_1}{dt} = -\alpha B S_1 + q S_2 + \varepsilon[1 - \beta S_1 I_1 - \sigma_I \beta S_1 I_2 - S_1] \\ \varepsilon \frac{dS_2}{dt} = \alpha B S_1 - q S_2 + \varepsilon[-\sigma_S \beta S_2 I_1 - \sigma_I \sigma_S \beta S_2 I_2 - S_2] \\ \varepsilon \frac{dI_1}{dt} = -\alpha B I_1 + q I_2 + \varepsilon\left[\beta S_1 I_1 + \sigma_I \beta S_1 I_2 - \frac{\gamma I_1}{1 + h I_1} - I_1\right] \\ \varepsilon \frac{dI_2}{dt} = \alpha B I_1 - q I_2 + \varepsilon\left[\sigma_S \beta S_2 I_1 + \sigma_S \sigma_I \beta S_2 I_2 - \frac{\gamma I_2}{1 + h I_2} - I_2\right] \\ \varepsilon \frac{dR_1}{dt} = -\alpha B R_1 + q R_2 + \varepsilon\left[\frac{\gamma I_1}{1 + h I_1} - R_1\right] \\ \varepsilon \frac{dR_2}{dt} = \alpha B R_1 - q R_2 + \varepsilon\left[\frac{\gamma I_2}{1 + h I_2} - R_2\right] \\ \varepsilon \frac{dB}{dt} = \rho(I_1 + I_2) - B \end{cases} \tag{3.3}$$

Applying the transformation of time $\tau = \frac{t}{\varepsilon}$, then the system on the fast time scale (3.4) is established:

$$\begin{cases} \frac{dS_1}{d\tau} = -\alpha B S_1 + q S_2 + \varepsilon[1 - \beta S_1 I_1 - \sigma_I \beta S_1 I_2 - S_1] \\ \frac{dS_2}{d\tau} = \alpha B S_1 - q S_2 + \varepsilon[-\sigma_S \beta S_2 I_1 - \sigma_I \sigma_S \beta S_2 I_2 - S_2] \\ \frac{dI_1}{d\tau} = -\alpha B I_1 + q I_2 + \varepsilon\left[\beta S_1 I_1 + \sigma_I \beta S_1 I_2 - \frac{\gamma I_1}{1 + h I_1} - I_1\right] \\ \frac{dI_2}{d\tau} = \alpha B I_1 - q I_2 + \varepsilon\left[\sigma_S \beta S_2 I_1 + \sigma_S \sigma_I \beta S_2 I_2 - \frac{\gamma I_2}{1 + h I_2} - I_2\right] \\ \frac{dR_1}{d\tau} = -\alpha B R_1 + q R_2 + \varepsilon\left[\frac{\gamma I_1}{1 + h I_1} - R_1\right] \\ \frac{dR_2}{d\tau} = \alpha B R_1 - q R_2 + \varepsilon\left[\frac{\gamma I_2}{1 + h I_2} - R_2\right] \\ \frac{dB}{d\tau} = \rho(I_1 + I_2) - B \end{cases} \tag{3.4}$$

3.2. Dynamical analysis on the fast subsystem

First, we analyze the dynamical behavior of fast subsystem. Let $\varepsilon \to 0$, system (3.4) becomes:

$$\begin{cases} \frac{dS_1}{d\tau} = -\alpha B S_1 + q S_2 \\ \frac{dS_2}{d\tau} = \alpha B S_1 - q S_2 \\ \frac{dI_1}{d\tau} = -\alpha B I_1 + q I_2 \\ \frac{dI_2}{d\tau} = \alpha B I_1 - q I_2 \\ \frac{dR_1}{d\tau} = -\alpha B R_1 + q R_2 \\ \frac{dR_2}{d\tau} = \alpha B R_1 - q R_2 \\ \frac{dB}{d\tau} = \rho(I_1 + I_2) - B \end{cases} \tag{3.5}$$

Let $S = S_1 + S_2, I = I_1 + I_2, R = R_1 + R_2$, from system (3.5), we get $S' = R' = I' = 0$, namely, in the sense of this fast system considering only information transmission, S, I and R are all constants. Then, system (3.5) can be reduced to the following four-dimensional system:

$$\begin{cases} \frac{dS_1}{d\tau} = -\alpha B S_1 + q(S - S_1) \\ \frac{dI_1}{d\tau} = -\alpha B I_1 + q(I - I_1) \\ \frac{dR_1}{d\tau} = -\alpha B R_1 + q(R - R_1) \\ \frac{dB}{d\tau} = \rho I - B \end{cases} \tag{3.6}$$

We can prove that this system has a unique positive equilibrium

$$E_{fast}^* = (S_1^*, I_1^*, R_1^*, B^*), \tag{3.7}$$

where $S_1^* = \frac{qS}{\alpha \rho I + q}, I_1^* = \frac{qI}{\alpha \rho I + q}, R_1^* = \frac{qR}{\alpha \rho I + q}, B^* = \rho I$. The stability of E_{fast}^* can also be proved as follows. By checking the Jacobian matrix of (3.6) at E_{fast}^* we know that the positive equilibrium is locally asymptotically stable. Considering that system (3.6) is a competitive system, the positive equilibrium is then globally asymptotically stable, and hence we have the following theorem.

Theorem 1. *The positive equilibrium E_{fast}^* of the fast subsystem (3.6) is globally asymptotically stable.*

3.3. Dynamical analysis on the slow subsystem

Then we analyze the dynamical behavior of the slow subsystem. Similarly, let $S = S_1 + S_2, I = I_1 + I_2, R = R_1 + R_2$, according to system (3.3), we have:

$$\begin{cases} \varepsilon \frac{dS}{dt} = \varepsilon[1 - \beta(S_1 + \sigma_S(S - S_1))(I_1 + \sigma_I I_2) - S] \\ \varepsilon \frac{dI}{dt} = \varepsilon\left[\beta(S_1 + \sigma_S(S - S_1))(I_1 + \sigma_I I_2) - \frac{\gamma I_1}{1 + h I_1} - \frac{\gamma(I - I_1)}{1 + h(I - I_1)} - I\right] \\ \varepsilon \frac{dR}{dt} = \varepsilon\left[\frac{\gamma I_1}{1 + h I_1} + \frac{\gamma(I - I_1)}{1 + h(I - I_1)} - R\right] \\ \varepsilon \frac{dB}{dt} = \rho I - B \end{cases}.$$

Substituting E^*_{fast} into the above system, and then the last equation of the above system is $\varepsilon \frac{dB}{dt} = 0$, so the B is constant in the sense of the slow system (3.3). Besides, B doesn't appear in the other equations, so we only need consider the first three equation of this model. Dividing both sides of it by ε, we can get that:

$$\begin{cases} \frac{dS}{dt} = 1 - \beta S I f(I) - S \\ \frac{dI}{dt} = \beta S I f(I) - \gamma I g(I) - I \\ \frac{dR}{dt} = \gamma I g(I) - R \end{cases}. \tag{3.8}$$

where

$$f(I) = \frac{(\sigma_I \alpha \rho I + q)(\sigma_S \alpha \rho I + q)}{(\alpha \rho I + q)^2}, \quad g(I)$$
$$= \frac{q}{\alpha \rho I + q + hqI} + \frac{\alpha \rho I}{\alpha \rho I + q + \alpha h \rho I^2}.$$

Considering the variable $R(t)$ does not feed back to the variables $S(t)$ and $I(t)$, we only need to consider the first two equations of system (3.8):

$$\begin{cases} \frac{dS}{dt} = 1 - \beta S I f(I) - S \\ \frac{dI}{dt} = \beta S I f(I) - \gamma I g(I) - I \end{cases}. \tag{3.9}$$

We can testify that $\Omega = \{(S, I) \in R_2^+ : S + I \leq 1\}$ is an attraction region of system (3.9), and this system always has disease-free equilibrium $E_0 = (1, 0)$. We firstly examine the local stability of E_0.

Theorem 2. *The disease-free equilibrium E_0 is locally asymptotically stable if $R_0 < 1$ and unstable if $R_0 > 1$. The bifurcation at $R_0 = 1$ is backward when $M_s > 0$; the bifurcation at $R_0 = 1$ is forward when $M_s < 0$, that is to say when $R_0 = 1, E_0$ is locally asymptotically stable if $M_s < 0$ and unstable if $M_s > 0$, where*

$$R_0 = \frac{\beta}{\gamma + 1},$$

$$M_s = a_1 - \beta^2 = \gamma h - (2 - \sigma_I - \sigma_s)\frac{\alpha \rho \beta}{q} - \beta^2. \tag{3.10}$$

Proof. By calculating the spectral radius of the next generation matrix for model (3.9), we can define and calculate the basic reproduction number R_0.

The Jacobian matrix concerned with the linearization of system (3.9) at E_0 is

$$J_{E_0} = \begin{pmatrix} -1 & -\beta \\ 0 & \beta - (\gamma + 1) \end{pmatrix}.$$

Therefore the eigenvalue of J_{E_0} are $\lambda_1 = -1$ and $\lambda_2 = (\gamma + 1)(R_0 - 1)$. Then, when $R_0 < 1$, all eigenvalues are negative; when $R_0 > 1, J_{E_0}$ has a positive eigenvalue. Thus the disease-free equilibrium E_0 of system (3.9) is unstable if $R_0 > 1$, and E_0 is locally asymptotically stable if $R_0 < 1$.

When $R_0 = 1$, the Jacobian matrix at E_0 has a zero eigenvalue. Hence E_0 is a nonhyperbolic equilibrium, and the linearization cannot determine its stability. Here, we use center manifold (Andronov et al., 1973; Shim, 1991) to analyze its stability.

Let $x = I$ and $y = S - 1$, system (3.9) is transformed to

$$\begin{cases} \frac{dx}{dt} = Q_1(x, y) \\ \frac{dy}{dt} = Q_2(x, y) \end{cases}, \tag{3.11}$$

where, $Q_1(x, y) = \beta(y + 1)xf(x) - \gamma xg(x) - x$ and $Q_2(x, y) = -y - \beta(y + 1)xf(x)$. So, the stability of E_0 of system (3.9) is equivalent to the stability of $(0, 0)$ of system (3.11). After the coordinate transformation $x = X$ and $y = Y - \beta X$, it becomes the standard form

$$\begin{cases} \frac{dx}{dt} = F(x, y) \\ \frac{dy}{dt} = -y + G(x, y) \end{cases}, \tag{3.12}$$

where $F(x, y) = -2(y - \beta x + 1)xf(x) - \gamma xg(x) - x$, $G(x, y) = \beta F(x, y) - \beta(y - \beta x + 1)xf(x) + \beta x$, and still writing it in terms of x and y just for the sake of simplicity. Algebraic calculations show that

$$F(0, 0) = 0, \quad \mathscr{D}F(0, 0) = 0,$$
$$G(0, 0) = 0, \quad \mathscr{D}G(0, 0) = 0.$$

Besides, functions $F(x, y)$ and $G(x, y)$ are both second differentiable in the first quadrant. According to the Center Manifold Theorem, system (3.11) has a locally C^2-class central manifold $y = c(x)(\|x\| < \delta)$. Since the stability of the zero solution of a system is often determined by the lower order terms, we can just consider the lower order terms of $Q_1(x, y), Q_2(x, y)$ and $c(x)$.

Expanding the functions $F(x, y)$ and $G(x, y)$ in the field of $(0, 0)$ through Taylor expansion, and substituting them into system (3.12), we get

$$\begin{cases} \frac{dx}{dt} = a_1 x^2 + 2\beta xy + \circ(r^3) \\ \frac{dy}{dt} = -y + b_1 x^2 + b_2 xy + \circ(r^3) \end{cases}, \tag{3.13}$$

where

$a_1 = 2\gamma h - 2(2 - \sigma_I - \sigma_s)\frac{\alpha \rho}{q} - 2\beta^2, b_1 = \beta a_1 + 2\left(\beta^2 + (2 - \sigma_I - \sigma_s)\frac{\alpha \rho}{q}\right)$, $b_2 = 2\beta(\beta + 1)$ and $r = \sqrt{x^2 + y^2}$. Similarly, $y = c(x)$ is expanded as

$$y = c(x) = c_0 + c_1 x + x_2 x^2 + c_3 x^3 + \dots = \Sigma_{k=0}^{\infty} c_k x^k.$$

Applying the invariance of center manifold, we have

$$-\beta x - \Sigma_{k=0}^{\infty} c_k x^k - b_1 x^2 - \beta x(\Sigma_{k=0}^{\infty} c_k x^k) + o(r^3)$$

By comparing the coefficients of the two ends of the above equation to the same power, we can get $c_0 = 0, c_1 = 0, c_2 = b_1$, that is

$$y = c(x) = b_1 x^2 + o(x^3).$$

Substituting it into the first equation of system (3.13), and we have

$$\frac{dx}{dt} = 2M_s x^2 + o(x^3)$$

where

$$M_s = \frac{a_1}{2} = \gamma h - (2 - \sigma_I - \sigma_s)\frac{\alpha \rho \beta}{q} - \beta^2.$$

So, the bifurcation at $R_0 = 1$ is backward when $M_s > 0$; the bifurcation at $R_0 = 1$ is forward when $M_s < 0$ (Broer, 1995; Castillo-Chavez and Song, 2004), that is to say, when $R_0 = 1, E_0$ is locally asymptotically stable if $M_s < 0$ and unstable if $M_s > 0$. This completes the proof. □

3.3.1. Global stability on the slow subsystem (3.8) with linear recovery term

Note that system (3.8) (or (3.9)) has high nonlinearity and it is complicated to calculate the endemic state. Given the complexity, we initially consider the special case where the recovery term is linear (i.e., $h = 0$).

Theorem 3. *Suppose $h = 0$, the slow system (3.9) has a unique positive equilibrium for $R_0 > 1$, and further the unique positive equilibrium is globally asymptotically stable for $R_0 > 1$ and $\sigma_I + \sigma_S > \frac{1}{2}$.*

Proof. When $h = 0$, if the slow system (3.9) has a positive equilibrium, denoted by (S_*, I_*), then we have

$$\begin{cases} 1 - \beta S_* I_* f(I_*) - S_* = 0 \\ \beta S_* I_* f(I_*) - (\gamma + 1)I_* = 0 \end{cases}. \tag{3.14}$$

From the second equation of (3.14), we have $S_* = \frac{\gamma+1}{\beta f(I_*)}$. Substituting into the first equation of (3.14) and simplifying yield

$$f(I_*) = \frac{1}{R_0 - \beta I_*} \tag{3.15}$$

Let $G(I) = \frac{1}{R_0 - \beta I}$, if the functions $f(I)$ and $G(I)$ intersect at $(0, 1)$, there is a $I_* \in (0, 1)$ that satisfies Eq. (3.15), that is to say, the slow system (3.9) has a positive equilibrium. Algebraic analysis shows that $f(I)$ decreases monotonically at $[0, 1]$, and $G(I)$ increases monotonically at $\left[0, \frac{1}{\gamma+1}\right)$ and $\left(\frac{1}{\gamma+1}, 1\right]$. Considering that $f(I) > 0$ for $I \in [0, 1]$, and $G(I) > 0$ for $I \in \left[0, \frac{1}{1+\gamma}\right)$ but $G(I) < 0$ for $I \in \left(\frac{1}{1+\gamma}, 1\right]$, we only need to analyze the intersection of function $f(I)$ and $G(I)$ at $\left[0, \frac{1}{1+\gamma}\right)$. We can testify that

$$f(0) < G(0) \iff R_0 < 1,$$
$$f(0) = G(0) \iff R_0 = 1,$$
$$f(0) > G(0) \iff R_0 > 1.$$

Combining the monotonicity of $f(I)$ and $G(I)$ and $\lim_{I \to \frac{1}{1+\gamma}} G(I) - f(I) = +\infty$, we have that $f(I)$ and $G(I)$ have a unique intersection at $[0, 1]$ when $R_0 > 1$; $f(I)$ and $G(I)$ have no intersection at $[0, 1]$ when $R_0 < 1$; and when $R_0 = 1$, the abscissa of the only intersection point of $f(I)$ and $G(I)$ is 0, i.e., $I = 0$, which is not positive. So that, when $h = 0$, if $R_0 > 1$, the slow system has a unique local equilibrium $E_1 = (S^*, I^*) = \left(\frac{1}{R_0} \frac{1}{f(I^*)}, I^*\right)$, where I^* is the only intersection of $f(I)$ and $G(I)$; if $R_0 \leq 1$, there is no local equilibrium.

To prove the stability of the unique local equilibrium E_1, we consider a Lyapunov function

$$V(S, I) = S - S^* \ln \frac{S}{S^*} + (I - I^* \ln(I)).$$

Then we have

$$\frac{dV}{dt} = 1 - S - S^* - \frac{S^*}{S} - (\gamma + 1)I + \beta S^* I f(I) - \beta S I^* f(I) + (\gamma + 1)I^*.$$

Recalling that $\beta S^* I^* f(I^*) + S^* = 1$ and $\gamma + 1 = \beta S^* f(I^*)$, we obtain

$$\frac{dV}{dt} = \beta S^* I^* f(I^*) \left[3 - \frac{S^*}{S} - \frac{S}{S^*} \frac{f(I)}{f(I^*)} - \frac{f(I^*)}{f(I)}\right]$$
$$+ \beta S^* I^* f(I^*) \left[\frac{If(I)}{I^* f(I^*)} - \frac{I}{I^*} - 1 + \frac{f(I^*)}{f(I)}\right] + 2S^* - S - \frac{S^{*2}}{S}.$$

Let $m(I) = If(I)$, we obtain

$$m'(I) = \frac{\sigma_I \sigma_S \alpha^3 \rho^3 I^3 + 3\sigma_I \sigma_S \alpha^2 \rho^2 qI^2 + [2(\sigma_I + \sigma_S) - 1]\alpha \rho q^2 I + q^3}{(\alpha \rho I + q)^3}$$
$$> 0$$

for all $I > 0$ and $\sigma_I + \sigma_S > \frac{1}{2}$. Hence, we have

$$[f(I^*) - f(I)][I^* f(I^*) - If(I)] \leq 0,$$

where the equality holds only when $I = I^*$, thus

$$\frac{If(I)}{I^* f(I^*)} - \frac{I}{I^*} - 1 + \frac{f(I^*)}{f(I)} = \left[\frac{I}{I^*} - \frac{If(I)}{I^* f(I^*)}\right]\left[\frac{I^* f(I^*)}{If(I)} - 1\right] \leq 0.$$

Furthermore, we have

$$\frac{S^*}{S} + \frac{S}{S^*} \frac{f(I)}{f(I^*)} + \frac{f(I^*)}{f(I)} \geq 3, \quad S + \frac{S^{*2}}{S} \geq 2S^*$$

for all $S, I > 0$, because the arithmetic mean is greater then or equal to the geometric mean. Therefore, $\frac{dV}{dt} \leq 0$ holds for $S, I > 0$. In addition, $\frac{dV}{dt} = 0$ holds only when $S = S^*$ and $I = I^*$, and E_0 is the only equilibrium of this systems on this plane. Therefore, the local equilibrium E_1 is globally asymptotically stable when $h = 0$ and $\sigma_I + \sigma_S > \frac{1}{2}$. This completes the proof. $\square$

Theorem 4. *Suppose $h = 0$, the disease-free equilibrium E_0 of system (3.9) is globally asymptotically stable for $R_0 \leqslant 1$, and it is unstable for $R_0 > 1$.*

Proof. First, according Theorem 2, we have that the disease-free equilibrium E_0 is unstable if $R_0 > 1$, and E_0 is locally asymptotically stable if $R_0 < 1$. Especially, when $R_0 = 1$ and $h = 0$, we have $M_s < 0$ holds true, which indicates E_0 is also locally asymptotically stable for $R_0 = 1$.

To prove global stability of E_0 when $R_0 \leq 1$, let's consider a Lyapunov function

$$V = I + S - \ln S.$$

In case of system (3.9), this Lyapumov function satisfies

$$\frac{dV}{dt} = 2 - \left(S + \frac{1}{S}\right) + (\gamma + 1)I(R_0 f(I) - 1).$$

Since the arithmetical mean is greater than or equal to the geometrical mean, the function $2 - (S + \frac{1}{S})$ is nonnegative for all $S, I > 0$. Consider the monotonicity of $f(I), f(I) \leqslant f(0) = 1$, then $R_0 f(I) - 1 \leq 0$ for all $0 \leqslant I \leqslant 1$. So that $\frac{dV}{dt} \leq 0$, for all $(S, I) \in \Omega$. Besides, $\frac{dV}{dt} = 0$ holds only when $S = 1$ and $I = 0$, and E_0 is the only equilibrium of this systems on this plane. Therefore the disease-free equilibrium E_0 is globally asymptotically stable when $R_0 \leq 1$. This completes the proof. $\square$

It can be seen from the above analysis that when the recovery term is linear, the basic reproduction number actually act as the threshold to distinguish whether the disease dies out or not for the slow system.

3.3.2. Global stability on the slow subsystem (3.8) with nonlinearly saturated recovery term

When the recovery term is nonlinearly saturated, that is $h \neq 0$, with help of numerical studies we investigate the existence and stability of positive equilibrium of system (3.9) (or (3.8)). Let $\hat{E}_1 = \left(\hat{S}, \hat{I}\right)$ be a positive equilibrium of system (3.9). From system (3.9), we can obtain

$$\hat{S} = \frac{1 + \gamma g\left(\hat{I}\right)}{\beta f\left(\hat{I}\right)}$$

and $\hat{I}$ is a solution of the equation $A(I) = B(I)$ for $0 < \hat{I} < 1$, where

$$A(I) = \frac{1}{1 + rg(I)}, \quad B(I) = \frac{1}{\beta f(I)} + I.$$

Then $A(0) = \frac{1}{1+r}, B(0) = \frac{1}{\beta}, A(1) = \frac{1}{1+rg(1)} < 1, B(1) = \frac{1}{\beta f(1)} + 1 > 1$. Let $H(I) = A(I) - B(I)$, then $H(1) = A(1) - B(1) < 0$.
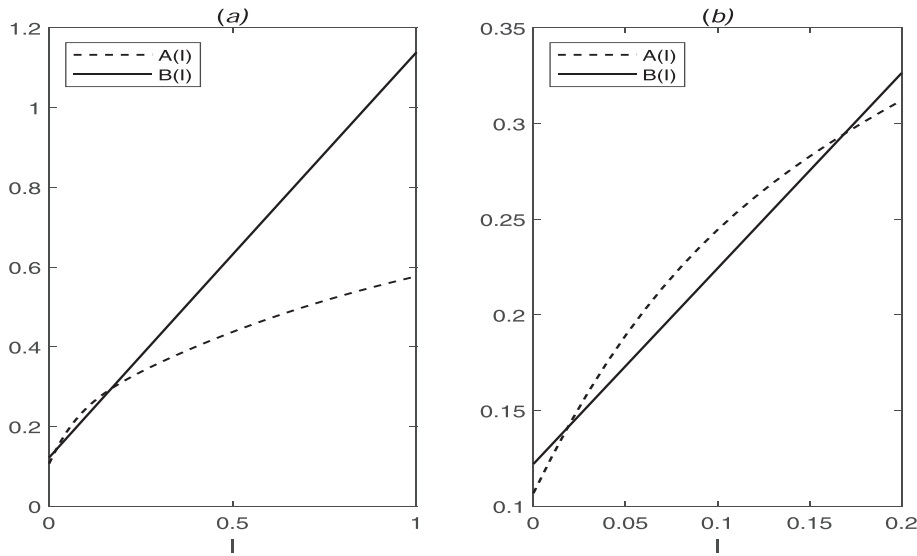
Fig. 2. (a): The curves of functions $A(I)$ and $B(I)$; (b): a partial magnification of the graph on (a), where $\alpha = 7.8964, \rho = 0.6786, h = 20.6671, q = 9.2084, \gamma = 8.3654$, $\sigma_S = 0.9312, \sigma_I = 0.7287, \beta = 8.1950$.

When $R_0 > 1$, we get $H(0) = A(0) - B(0) = \frac{1}{\beta}(R_0 - 1) > 0$. Combing $H(1) < 0$, according to the zero point theorem, we get that $H(I)$ has at least one zero point on $[0, 1]$, i.e., the slow system (3.9) has at least one endemic equilibrium.

When $R_0 < 1, H(0) < 0$. Denote $H_{max} = \max\limits_{0 \leqslant I \leqslant 1}\{H(I)\}$. When $H_{max} < 0$, equation $A(I) = B(I)$ has no solution on $[0, 1]$, so the slow system (3.9) has no positive equilibrium. For $H_{max} > 0$, there must be a $\widetilde{I} \in (0, 1)$, such that $H(\widetilde{I}) > 0$, so $H(0)H(\widetilde{I}) < 0$ and $H(\widetilde{I})H(1) < 0$. According to the zero point theorem, $H(I)$ has at least two zero point, one is in the interval of $(0, \widetilde{I})$ and the other in $(\widetilde{I}, 1)$, i.e., the system has at least two positive equilibriums.

From what has been shown above, we have the following results.

Theorem 5. *When $R_0 < 1$, the slow subsystem (3.9) has at least two positive equilibria for $H_{max} > 0$; there is no positive equilibrium for the slow subsystem (3.9) for $H_{max} < 0$. When $R_0 > 1$, the slow subsystem (3.9) has at least one positive equilibrium.*

We numerically plot the curve of functions $A(I)$ and $B(I)$ with respect to I as shown in Fig. 2. It shows that there are two intersection points of functions $A(I)$ and $B(I)$, which indicates this system has two positive equilibriums, that is a case of Theorem 5 for $R_0 < 1$, and $H_{max} > 0$. Further, we have the following dynamic behavior of the slow system in this case.

Theorem 6. *When $R_0 < 1$ and $H_{max} < 0$, the disease-free equilibrium E_0 is globally asymptotically stable.*

Proof. Let's consider a Lyapunov function

$$V = I + S + \int_0^I \frac{1}{\beta \tau f(\tau)} d\tau.$$

In the case of system (3.9), this Lyapumov function satisfies

$$\frac{dV}{dt} = 1 - [1 + \gamma g(I)]I - \frac{1 + \gamma g(I)}{\beta f(I)}$$
$$= [1 + \gamma g(I)] \left[\frac{1}{1 + \gamma g(I)} - \left(I + \frac{1}{\beta f(I)} \right) \right].$$

If $H_{max} < 0$, then we have $\frac{1}{1 + \gamma g(I)} < I + \frac{1}{\beta f(I)}$ for $I \in [0, 1]$, indicating $\frac{dV}{dt} \leq 0$. And $\frac{dV}{dt} = 0$ holds only when $S = 1$ and $I = 0$. Moreover, we know that E_0 is locally asymptotically stable for $R_0 < 1$, then we can get the disease-free equilibrium E_0 is globally asymptotically stable. That completes proof. $\square$

To numerically show the dynamic behaviors, we plot solutions of the slow system (3.9). Fig. 3(a) shows solutions of the slow system (3.9) for $R_0 < 1$ and $H_{max} > 0$, which illustrates that the solutions with lower initial values $I(0)$ converge to E_0, whereas the solutions with larger initial values $I(0)$ converge to a positive equilibrium. Fig. 3(c) shows that if there is only one positive equilibrium for $R_0 > 1$, solutions with arbitrary initial values $I(0)$ converge to the positive equilibrium.

Remark 1. When $h \neq 0, R_0$ is no longer the threshold to distinguish whether the disease dies out or not. And the slow subsystem (3.9) may occur backward bifurcation according to Theorem 2. However, M_s, (3.10), is related to information transmission parameters, and

$$\frac{\partial M_s}{\partial \sigma_I} > 0, \frac{\partial M_s}{\partial \sigma_S} > 0, \frac{\partial M_s}{\partial q} > 0 \frac{\partial M_s}{\partial \alpha} < 0, \frac{\partial M_s}{\partial \rho} < 0,$$

so M_s may decrease to below 0 by increasing α or ρ, or decreasing σ_I, σ_S or q. That indicates we can increase the information transmission rate, the changing rate of the coverage number of daily news items, or decrease the adjustment factors of transmission rate, the rate of loss consciousness to avoid the occurrence of backward bifurcation.

It is also known that the dynamics of the fast and slow subsystem are useful to gain insights into the dynamics of the full system by applying tools in perturbation theory (Fenichel, 1979; Gandolfi et al., 2015).

4. Dynamical analysis of the full system

In this chapter, we begin by analyzing the dynamic behaviors of the full system (2.1) and examine the similarities between these dynamic behaviors of the full system and the slow system (3.8) (or (3.9)). Since variables R_1 and R_2 are decoupled with the other
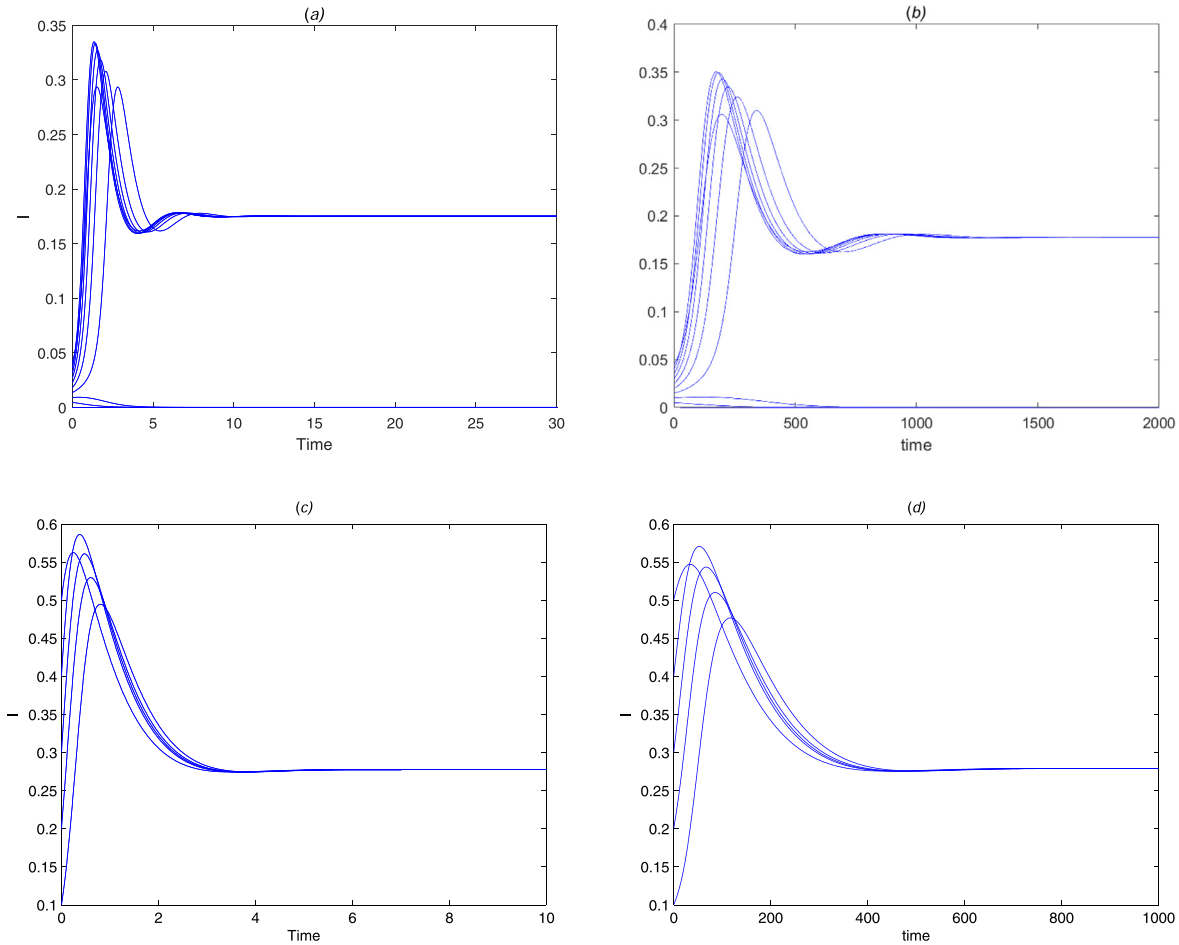
Fig. 3. (a): Solutions to the slow system (3.9),where $\alpha = 7.8964, \rho = 0.6786, h = 20.6671, q = 9.2084, \gamma = 8.3654, \sigma_S = 0.9312, \sigma_I = 0.8287, \beta = 8.2950$ and $R_0 = 0.8857$. (b): Solutions to the full system (4.16),where $d = 0.0934, \mu = 0.0072$, the value of other parameters after parameter transformation (3.2) is the same as the value of (a), and $R_{0f} = 0.8857, R_{hf} = 0.1480$. (c): Solutions to the slow system (3.9), where $\alpha = 8.5316, \rho = 0.7068, h = 21.1662, q = 9.7470, \gamma = 6.8296, \sigma_S = 0.9501, \sigma_I = 0.7330, \beta = 8.6402$ and $R_0 = 1.1035$. (d): Solutions to the full system (4.16), where $d = 0.0949, \mu = 0.0077$, the value of other parameters after parameter transformation (3.2) is the same as the value of (c) and $R_{0f} = 1.1035 > 1, R_{hf} = 0.1671$.

five equations of model (2.1), we only need to consider the following model:

$$
\begin{cases}
\frac{dS_1}{dt} = \mu - \beta S_1 I_1 - \sigma_I \beta S_1 I_2 - \mu S_1 - \alpha B S_1 + q S_2 \\
\frac{dS_2}{dt} = -\sigma_S \beta S_2 I_1 - \sigma_I \sigma_S \beta S_2 I_2 - \mu S_2 + \alpha B S_1 - q S_2 \\
\frac{dI_1}{dt} = \beta S_1 I_1 + \sigma_I \beta S_1 I_2 - \frac{\gamma I_1}{1 + h I_1} - \mu I_1 - \alpha B I_1 + q I_2 \\
\frac{dI_2}{dt} = \sigma_S \beta S_2 I_1 + \sigma_S \sigma_I \beta S_2 I_2 - \frac{\gamma I_2}{1 + h I_2} - \mu I_2 + \alpha B I_1 - q I_2 \\
\frac{dB}{dt} = \rho(I_1 + I_2) - dB
\end{cases}
\tag{4.16}
$$

We can testify that the feasible region of model (4.16) is

$$
\Gamma = \left\{ (S_1, S_2, I_1, I_2, B) \in R_+^5 : 0 < S_1 + S_2 + I_1 + I_2 \leqslant 1, 0 < B \leqslant \frac{\rho}{d} \right\},
$$

which is a positively invariant set. A disease-free equilibrium $E_{0f} = (1, 0, 0, 0, 0)$ is always feasible. By calculating the spectral radius of the next generation for model (4.16), we get the basic reproduction number of this model is $R_{0f} = \frac{\beta}{\mu + \gamma}$, where R_{0f} is the expected number of secondary cases produced, in a completely susceptible population, by a typical infective individual (Dreessche and Watmough, 2002).

Similarly we can investigate the stability of the disease-free equilibrium E_{0f}, the bifurcation at E_{0f} for $R_{0f} = 1$, and we can also

analyze the persistence of the full system (4.16) for $R_{0f} > 1$. In the following we only give the main conclusions and the detailed proof processes are given in Appendix A.

Theorem 7. *If $R_{0f} < 1$, the disease-free equilibrium E_{0f} of system (4.16) is locally asymptotically stable; if $R_{0f} > 1$, the disease-free equilibrium E_{0f} is unstable. The bifurcation at $R_{0f} = 1$ is backward if $M_f > 0$, and the bifurcation is forward if $M_f < 0$, where*

$$
M_f = \left(h\gamma - \frac{\beta^2}{\mu} \right) \frac{d}{\rho} (\mu + q)(\beta + q)
$$
$$
- [(2 - \sigma_I - \sigma_S)q + (1 - \sigma_I)\mu + (1 - \sigma_I \sigma_S)\beta]\alpha\beta.
\tag{4.17}
$$

Further, if $R_{0f} < R_{hf}$, the disease-free equilibrium E_{0f} of system (4.16) is globally asymptotically stable, where $R_{hf} = \frac{\mu(1+h)+\gamma}{(\mu+\gamma)(1+h)}$.

Theorem 8. *When $R_{0f} > 1$, system (4.16) is uniformly persistent, that is, there is a constant $\eta > 0$, and for all initial values $(S_1(0), S_2(0), I_1(0), I_2(0), B(0)) \in Int\left(R_+^5 \right)$, the solution of the system satisfies*

$$
\liminf_{t \to \infty} (S_1(t), S_2(t), I_1(t), I_2(t), B(t)) > (\eta, \eta, \eta, \eta, \eta).
$$

It is worthy noticing the similarity between the dynamic behaviors of the slow system (3.9) and the full system (4.16). The basic reproduction number R_{0f} of the full model (4.16) and R_0 of the slow model (3.9) are equivalent, because the parameters in model (3.9) are obtained by parameter transformation (3.2). On the basis of Theorems 2 and 7, we can conclude that the locally stability of disease-free equilibrium E_0 of the slow subsystem (3.9) is equivalent to the locally stability of disease-free equilibrium E_{0f} of the full system (4.16) except the situation $R_0 = R_{0f} = 1$, where bifurcation may occur, which will be discussed later.

When the recovery term is linear, the basic reproduction number actually act as the threshold to distinguish whether the disease dies out or not for the slow system and the full system on the basis of Theorem 4 and Theorem 7. When $h \neq 0$, the basic reproduction number R_0 (or R_{0f}) is no longer the threshold to distinguish whether the disease dies out or not for the slow system (or the full system). The full system occurs backward bifurcation at E_{0f} for $R_{0f} = 1$ and $M_f > 0$ on the basis of Theorem 7; the slow system occurs backward bifurcation at E_0 for $R_0 = 1$ and $M_s > 0$ on the basis of Theorem 2. It is interesting to notice that the conditions
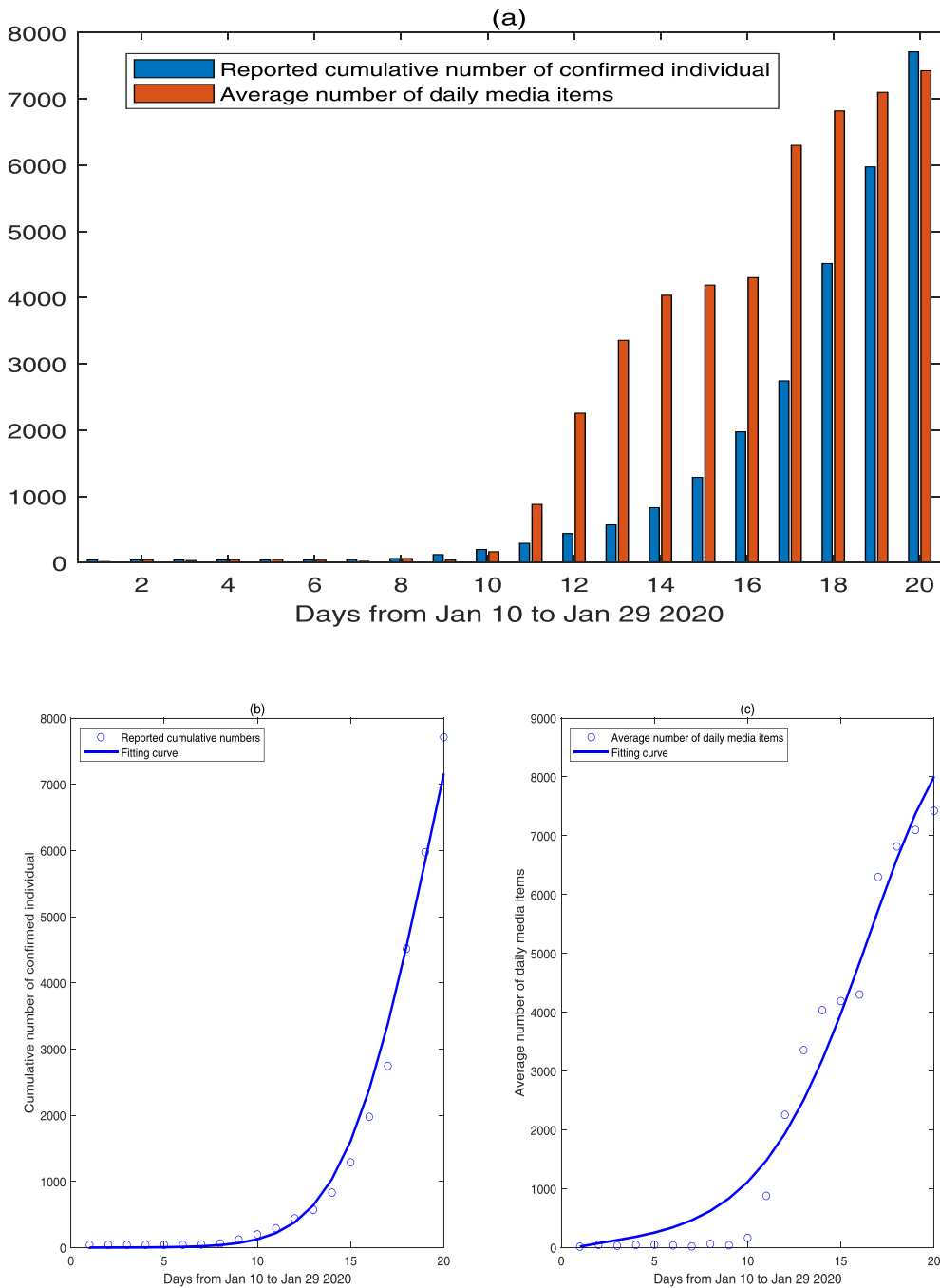

Fig. 4. (a):The reported cumulative number of confirmed cases and the average daily number of media items from January 10 to 29. (b) and (c): Data fitting for the data from January 15 to 29, 2020. The circles in (b) and (c) represent the cumulative number of confirmed cases, the average daily number of media items, from January 10 to 29 respectively. The curves are the best fitting curves of model (4.16) to these data.

Table 1
Estimated initial values of variables and parameters for system (4.16).

Variables	Description	Initial value	Resource
$S_1(0)$	Unconscious susceptible population	0.9999	LS
$S_2(0)$	Conscious susceptible population	739/11081000	Zhou et al. (2020)
$I_1(0)$	Unconscious infected population	1.0000×10^{-5}	LS
$I_2(0)$	Conscious infected population	41/11081000	Data
B	Media items	16.3	Data
Parameters	**Description**	**Value**	**Resource**
μ	Natural death rate/Birth rate	0	Assumed
β	Probability of transmission from I_1 to S_1	0.4555	LS
α	Propagation rate of consciousness	2.0981×10^{-5}	LS
q	The rate of losing consciousness	0.0010	LS
γ	Recovery rate of infected individuals	0.1400	LS
ρ	Media reporting rate of number of infected population	5.1753×10^6	LS
θ	The adjustment factor of media reporting rate of number of I_2	1	Assumed
d	The spontaneous disappearance rate of media reports	0.5000	LS
h	Non-negative parameter	4.9891×10^{-12}	LS
σ_I	the reduction factors in transmission rate when infection occurs between I_2 and S_1	0.2398	LS
σ_S	the reduction factors in transmission rate when infection occurs between I_1 and S_2	0.2398	LS

for branching in the slow system (3.9) ($M_s > 0$) and the full system (4.16) ($M_f > 0$) are also equivalent on the basis of the time variation between information dissemination and epidemiological and demographic process ($\varepsilon = \frac{\mu}{d} \ll 1$). Especially, M_f is related to information transmission parameters, and

$$\frac{\partial M_f}{\partial \sigma_I} > 0, \frac{\partial M_f}{\partial \sigma_S} > 0, \frac{\partial M_f}{\partial \alpha} < 0,$$

and

$$\frac{\partial M_f}{\partial \rho} < 0, \frac{\partial M_f}{\partial q} > 0$$

for $M_f > 0$, so we may also decrease M_f to below 0 by increasing α or ρ, or decreasing σ_I, σ_S or q, which are similar with the situations of the slow system (3.9) on the basis of Remark 1. See Appendix B for details. Again we can increase the information transmission rate, the changing rate of the coverage number of daily news items, or decrease the adjustment factors of transmission rate, the rate of loss of consciousness to avoid the occurrence of backward bifurcation.

The disease-free equilibrium E_0 of the slow system (3.9) is globally asymptotically stable for $R_0 < 1$ and $H_{max} < 0$ on the basis of Theorem 6. The disease-free equilibrium E_{0f} of the full system (4.16) for $R_{0f} < R_{hf}$ is globally asymptotically stable on the basis of Theorem 7. It is easy to testify that if $R_{0f} < R_{hf}$, we can conclude $H_{max} < 0$ holds true. In fact, if $R_{0f} < R_{hf}$, and applying the parameter transformation (3.2) on this, similarly, the parameters of subsequent models are still recorded as the original parameters, we can get $\frac{\beta}{1+\gamma} < \frac{1+\gamma\frac{1}{1+h}}{1+\gamma}$, then $\frac{1}{\beta} > \frac{1}{1+\gamma\frac{1}{1+h}}$. Since both $f(I)$ and $g(I)$ are monotonically decreasing in $[0, 1]$, we get

$$H(I) = A(I) - B(I) = \frac{1}{1 + \gamma g(I)} - \left[\frac{1}{\beta f(I)} + I\right] \leqslant \frac{1}{1 + \gamma g(1)} - \frac{1}{\beta f(0)}$$

$$= \frac{1}{1 + \gamma g(1)} - \frac{1}{\beta} < \frac{1}{1 + \gamma g(1)} - \frac{1}{1 + \gamma\frac{1}{1+h}}.$$

Due to $\frac{1}{1+h} < g(1)$, we have $H(I) < 0$ for $I \in [0, 1]$, which implies $H_{max} < 0$. However, $H_{max} < 0$ does not necessarily mean $R_{0f} < R_{hf}$ holds true. Moreover, we only obtained the uniform persistence for $R_{0f} > 1$, we do not know the existence of endemic states for $R_{hf} < R_{0f} < 1$, which indicates that we got the relatively strict/strong condition under which the disease-free equilibrium of the full system is globally asymptotically stable. This comparison implies that based on fast-slow system theory we can obtain the detailed dynamics of the slow system, which represents the dynam-

ics of the full system, while for the full system, it is challengeable to examine the complex and rich dynamics due to high dimension. Hence, it is reasonable to examine the dynamics of the slow system rather than directly investigating the full system.

Numerical simulations are used to further illustrate the similarity of dynamic behavior between the full system (4.16) and the slow system (3.9). To illustrate the existence of the backward bifurcation for the full system and the slow system, we plot solutions of the slow system and the full system with equivalent parameters for $R_{hf} < R_{0f} = R_0 < 1$ and $H_{max} > 0$, shown in Fig. 3(a) and (b). It shows that solutions with relatively low initial values of $I(0)$ converge to 0, whereas solutions with relatively large initial values of $I(0)$ converge to a similar positive level of infection proportion both for the slow system and the full system. It's worth noting that solutions of two systems converge with very different convergent speed. In particular, solutions of the slow subsystem quickly converge to the equilibrium, while solutions of the full system slowly converge. Moreover, Fig. 3(c) and (d) show that for $R_{0f} > 1$ (or $R_0 > 1$), both solutions of the slow system and the full system converge to almost the same positive equilibrium but with very different convergent speed.

5. A case study

In this subsection we tried to parameterize the proposed model with surveillant data and news items data on early stage of COVID-19 infection in mainland China, and numerically investigate the media impact of COVID-19 infection. We obtained the reported cumulative number of confirmed COVID-19 cases in China from the National Health Commission of the People's Republic of China (Data). Although the first case was reported in December 2019, a new confirmed case was not reported until 10 January 2020, we used data from 10 January to 29 January, 2020, as shown in Fig. 4 (a). The case data was released and analyzed anonymously. We also obtained daily weighted average number of media items from 7 major websites during January 10–29, 2020, as in Zhou et al. (2020), which is shown in Fig. 4(a).

In the initial stage of the epidemic, we assume that the total population is Wuhan residents, the conscious susceptible population is the isolated susceptible population, the conscious infected population is the reported confirmed population and no individual was recovered. We further assume $\mu = 0$ because of the short epidemic time scale in comparison to the demographic time scale. We used the Least Square Method to fit the parameters in model (4.16) to study the effects of information transmission about disease

caused by media coverage on COVID-19 infection. The fitting results are shown in Fig. 4(b) and (c), and the estimated parameter values with sources of other parameters are given in Table 1. Based on the above-mentioned parameter estimations, we then calculated R_{0f} as 3.25. Note that this estimation agrees with those estimations based on likelihood-based methods (Imai et al., 2020; Li et al., 2020), while it is less than those estimated levels based on the dynamic models without considering media impact (Tang et al., 2020; Ying et al., 2020). This implicitly indicates information transmission greatly leads to the new infections decline by influencing individuals's behaviour changes.

To further examine the possible impact of information transmission on disease infections, we plotted the prevalence $(I_1(t) + I_2(t))$ with different values of α, q, σ_I and ρ, as shown in Fig. 5 and the contour plots of the peak size of the outbreak $(I_1(t) + I_2(t))$ with respect to α, ρ and σ_I and q, as shown in Fig. 6, to examine the dependence of the peak size of the infection on information transmission. Those all show that the larger α or ρ is (or the smaller q or σ_I is), the lower the peak size is. It indicates that increasing the information transmission rate (α), the strengthening the intensity of media report (ρ), or decreasing the loss rate of consciousness (q), the adjustment factor for transmission rate (σ_I), will effectively reduce the peak size. This illustrates that information transmission can mitigate the COVID-19 transmission, which calls for the importance of media coverage when facing the outbreak of emerging infectious diseases like COVID-19 pandemic.

Note that directly fitting the proposed model to data may induce a bias since our model does not consider the infection induced by the asymptomatic infected individuals, which were proven to be extremely important for epidemiology of COVID-19 (Amaral et al., 2021; Castro et al., 2020). We then simply extend our model by including a compartment of asymptomatic infected individuals (see detailed model equations in C) and data fitting gives the similar parameter estimations and a slightly great basic reproduction number as 3.30. This indicates that ignoring asymptomatic individuals may underestimate the COVID-19 infection. We mention here that the inclusion of asymptomatic individuals leads to a higher dimensional system, which is difficult to analyze theoretically, and we leave this for further study.

6. Conclusion and discussion

Media coverage has great influence on both information transmission about disease and the propagation of the infectious disease. It's important to understand the effects of information
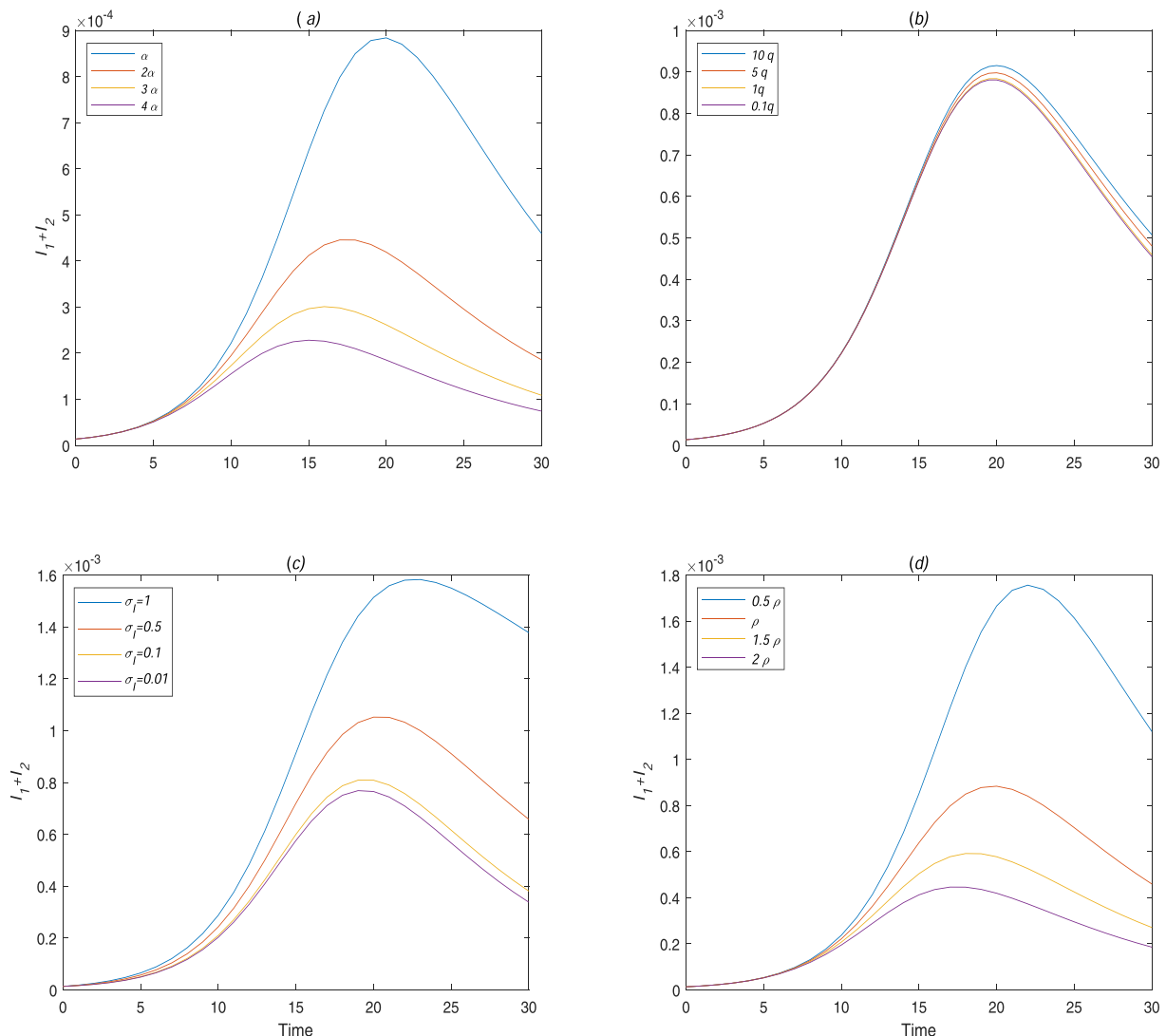

Fig. 5. Variation in the total number of infected individuals $(I_1(t) + I_2(t))$ with parameters α (a), q (b), σ_I (c) and ρ (d), respectively. The corresponding parameter values are shown in Table 1.
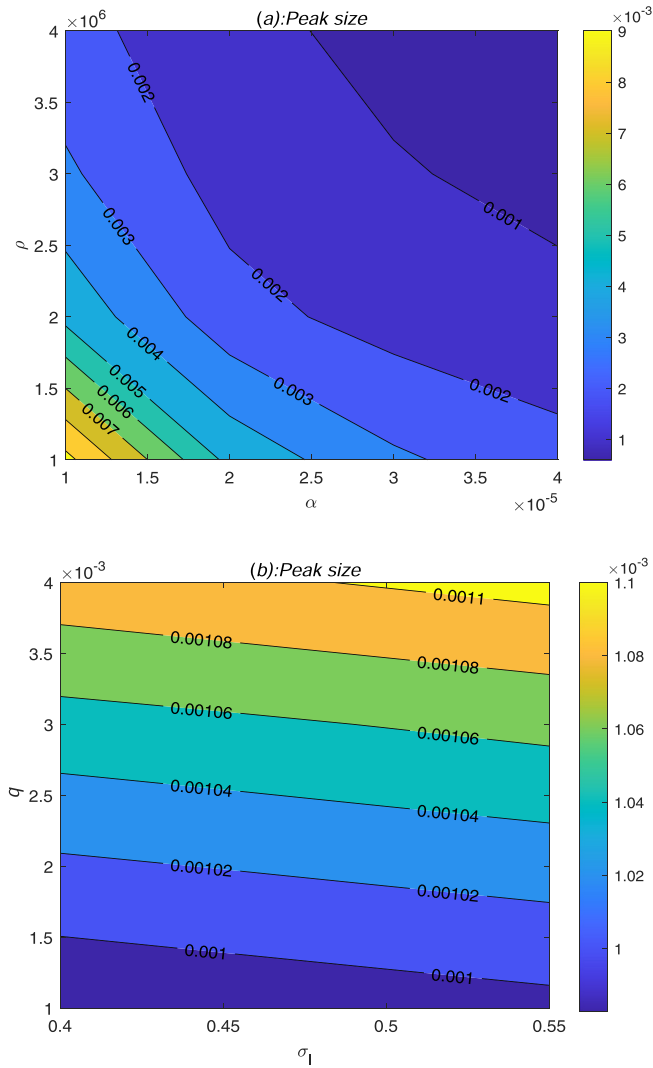
Fig. 6. Contour plots of the peak size of the outbreak $I_1(t) + I_2(t)$ with respect to α and p (a), and σ_I and q (b), respectively. The corresponding parameter values are shown in Table 1.

transmission caused by the media coverage during epidemic, so as to propose public health communication strategies and disease mitigation measures. To investigate the interaction of information transmission and disease transmission, we proposed the multi-scale model which explicitly models both the disease transmission with saturated recovery rate and information transmission and used the theory of the slow-fast system to analyze this model. When the recovery term is linear, we obtained the conditions for the existence and stability of a positive equilibrium theoretically, and analysed the impact of disease transmission on the prevalence of infection through numerical simulation. When the recovery term is nonlinearly saturated, R_0 is no longer the threshold to distinguish whether an outbreak takes out or not, and our model may occur a so-called backward bifurcation.

Especially, we establish slow-fast system by introducing a sufficiently small quantity ($\frac{\mu}{d} \ll 1$), which is determined by death rate and media wading rate, on the basis of slow dynamics of demographic process (associated with relatively small value of μ) and fast dynamics of information dissemination (associated with relatively large value of d), which is more natural and reasonable compared with the method in literature (Samanta and Chattopadhyay,

2014), introducing an infinitely small quantity directly. Besides, in this paper, the dynamic behaviors of the slow system and the full system are both analyzed, which are similar, but the convergent speed towards the equilibrium is different. This indicates that, for this multi-scale model (if complicated), the basic dynamic behavior can be obtained just by simulating the slow system with data, which can save calculational costs and obtain the relatively detailed theoretical results.

In this paper, through analyzing the existence and stability of positive equilibriums and the existence of backward bifurcation, we confirmed that when the recovery term is linear, the information transmission does not change the outbreak of disease, but affects the prevalence of infection; when the recovery term is nonlinearly saturated, backward bifurcation may occur, but the backward bifurcation can be avoided by controlling information transmission. Further, we parameterized the proposed model on the basis of the COVID-19 case data and data on news items in mainland China, and estimated the basic reproduction number to be 3.25. Numerical analyses suggest improving information transmission about disease induced by media coverage is an effective way to mitigate COVID-19 infection by reducing peak size during the early stage of the COVID-19 pandemic. It is worth noting that although the proposed nonlinear recovery function can describe the saturated effect due to the limitation of medical resources, it may not represent the case that people would die more likely once the health care system gets overwhelmed (say SARS-CoV-2 infection in some country). We then need to extend it by further proposing the piecewise smooth function to represent, say, there is a threshold for the number of infected individuals I_c such that saturated recovery function is feasible for $I(t) < I_c$, while linear recovery function is satisfied for otherwise. The piecewise smooth function will bring the difficulties in analyzing the global dynamics of the system and we leave this for future work.

CRediT authorship contribution statement

Tangjuan Li: Methodology, Software, Writing - original draft. **Yanni Xiao:** Conceptualization, Methodology, Supervision, Validation, Writing - review & editing.

Declaration of interest

The authors declare no competing financial interests.

Acknowledgments

Appendix A. The proof of all Theorem in Section 4

A.1. The proof of Theorem 7

Proof. By checking the Jacobian matrix at E_{0f}, we can examine the local stability of the disease-free equilibrium E_{0f}.

Then we analyze the bifurcation at $R_{0f} = 1$. Let $X = (S_1, S_2, I_1, I_2, B)^T = (x_1, x_2, x_3, x_4, x_5)^T$, where $(.)^T$ is the transpose of the matrix, so model (4.16) can be denoted as $\dot{X} = F = (f_1, f_2, f_3, f_4, f_5)^T$.

The linearization matrix of model (4.16) around E_{0f} when $R_{0f} = 1$ is

$$J_{E_{0f}} = \begin{pmatrix} -\mu & q & -\beta & -\sigma_I\beta & -\alpha \\ 0 & -\mu-q & 0 & 0 & \alpha \\ 0 & 0 & 0 & \sigma_I\beta+q & 0 \\ 0 & 0 & 0 & -\gamma-\mu-q & 0 \\ 0 & 0 & \rho & \rho & -d \end{pmatrix}.$$

It is clear that 0 is a simple eigenvalue of $J_{E_{0f}}$, and all other eigenvalues are negative, so E_{0f} is the non–hyperbolic equilibrium point. The left and right eigenvalues of $J_{E_{0f}}$ are denoted as v and w respectively, where $v = (v_1, v_2, v_3, v_4, v_5)^T, w = (w_1, w_2, w_3, w_4, w_5)^T$. Algebraic calculations show that

$$v_1 = 0, v_2 = 0, v_3 = \frac{\gamma+\mu+q}{\sigma_I\beta+q}v_4, v_5 = 0;$$

$$w_1 = -\left(\frac{\beta d}{\rho\mu} + \frac{\alpha}{\mu+q}\right)w_5, w_2 = \frac{\alpha}{\mu+q}w_5, w_3 = \frac{d}{\rho}w_5, w_4 = 0,$$

where, $w_5 > 0$. One can choose w_5 and v_4 satisfy:

$$v_4 w_5 = \left(\frac{\gamma+\mu+q}{\sigma_I\beta+q}\frac{d}{\rho}\right)^{-1} > 0,$$

such that $vw = 1$.

Let $\hat\gamma = \beta - \mu$ and $\phi = \hat\gamma - \gamma$, then $R_0 < 1$ if and only if $\phi < 0$. According to Theorem 4.1 in Castillo-Chavez and Song (2004), the local dynamic behavior near $R_{0f} = 1$ is determined by the following constants a and b:

$$a = \sum_{i,j,k=1}^{5} v_k w_i w_j \frac{\partial^2 f_k}{\partial x_i \partial x_j}(E_{0f}, 0),$$

$$b = \sum_{i,k=1}^{5} v_k w_i \frac{\partial^2 f_k}{\partial x_i \partial \phi}(E_{0f}, 0).$$

In terms of a and b, we just have to find the nonzero partial derivative of f_3 and f_4 at E_{0f} when $R_{0f} = 1$ and $\phi = 0$. Algebraic calculations show that

$$\frac{\partial^2 f_3}{\partial x_1 \partial x_3}(E_{0f}, 0) = \beta, \frac{\partial^2 f_3}{\partial x_1 \partial x_4}(E_{0f}, 0) = \sigma_I\beta, \frac{\partial^2 f_3}{\partial x_3 \partial x_5}(E_{0f}, 0) = -\alpha,$$

$$\frac{\partial^2 f_3}{\partial^2 x_3}(E_{0f}, 0) = 2h\gamma, \frac{\partial^2 f_4}{\partial x_2 \partial x_3}(E_{0f}, 0) = \sigma_S\beta, \frac{\partial^2 f_4}{\partial x_2 \partial x_4}(E_{0f}, 0) = \sigma_S\sigma_I\beta,$$

$$\frac{\partial^2 f_4}{\partial x_3 \partial x_5}(E_{0f}, 0) = \alpha, \frac{\partial^2 f_4}{\partial^2 x_4}(E_{0f}, 0) = 2h\gamma;$$

$$\frac{\partial^2 f_3}{\partial x_3 \partial \phi}(E_{0f}, 0) = \frac{1}{h^2}, \frac{\partial^2 f_3}{\partial x_4 \partial \phi}(E_{0f}, 0) = \frac{1}{h^2}.$$

All other partial derivative of f_3 and f_4 are zero. So, we can get that

$$b = \frac{1}{h^2}v_3 w_3 = \frac{1}{h^2}\frac{d}{\rho}\frac{\gamma+\mu+q}{\sigma_I\beta+q}v_4 w_5 > 0;$$

$$a = v_3(2\beta w_1 w_3 - 2\alpha w_3 w_5 + 2h\gamma w_3^2) + v_4(2\sigma_s\beta w_2 w_3 + 2\alpha w_3 w_5) = 2\frac{d}{\rho(\sigma_I\beta+q)(\mu+q)}v_4 w_5^2$$

$$\left\{\left(h\gamma - \frac{\beta^2}{\mu}\right)\frac{d}{\rho}(\mu+q)(\beta+q) - [(2-\sigma_I-\sigma_S)q + (1-\sigma_I)\mu + (1-\sigma_I\sigma_S)\beta]\alpha\beta\right\} \doteq 2\frac{d}{\rho(\sigma_I\beta+q)(\mu+q)}v_4 w_5^2 M_f.$$

We have that if $M_f > 0$, then $a > 0$; if $M_f < 0$, then $a < 0$. So we get the bifurcation at $R_{0f} = 1$ is backward when $M_f > 0$; the bifurcation at $R_{0f} = 1$ is forward when $M_f < 0$. Especially, when $h = 0, M_f < 0$ must hold, so the bifurcation at $R_{0f} = 1$ is forward when $h = 0$.

To testify the globally stability of E_{0f}, let's consider a continuous differentiable and positive definite Lyapunov function

$$V = I_1 + I_2.$$

So the derivative along system (4.16) is:

$$\frac{dV}{dt} = \beta(S_1 + \sigma_S S_2)(I_1 + \sigma_I I_2) - \frac{rI_1}{1+hI_1} - \frac{rI_2}{1+hI_2} - \mu(I_1+I_2)$$

$$\leqslant (I_1+I_2)(\mu+\gamma)\left(R_{0f} - \frac{\mu+\gamma\frac{1}{1+h}}{\mu+\gamma}\right)$$

$$= (I_1+I_2)(\mu+\gamma)(R_{0f} - R_{hf}).$$

Then, if $R_{0f} < R_{hf}, \frac{dV}{dt} \leq 0$. In addition, $\frac{dV}{dt} = 0$ holds only when $I_1 = I_2 = 0$, so the maximum compact invariant subset of set $\frac{dV}{dt} = 0$ in feasible region Γ is $(I_1, I_2) = (0,0)$. According to LaSalle's invariant set principle, when $t \to \infty$, we have $(I_1(t), I_2(t)) \to (0,0)$.

Since $\lim_{t\to\infty}I_1(t) = 0$ and $\lim_{t\to\infty}I_2(t) = 0$, for sufficiently small ε, there are constants T_1 and T_2, so that when $t > T_1, I_1(t) \leqslant \varepsilon$ and $t > T_2, I_2(t) \leqslant \varepsilon$. According to the last equation of model (4.16), we get that $\frac{dB}{dt} \leqslant \rho(\varepsilon + \theta\varepsilon) - dB$ when $t > max\{T_1, T_2\}$. Then from the comparison principle and non-negativity of solutions, we have $\lim_{t\to\infty}B(t) = 0$.

Similarly, $\lim_{t\to\infty}S_2(t) = 0, \lim_{t\to\infty}S_1(t) = 1$.

So, if $R_{0f} \leqslant R_{hf}$, the solution from Γ for model (4.16), approaches E_{0f} as $t \to \infty$. That is, when $R_{0f} < R_{hf}, E_{0f}$ is globally asymptotically stable. That completes the proof. $\square$

A.2. The proof of Theorem 8

Proof. Define the set

$$X = \{(S_1, S_2, I_1, I_2, B)|S_1 \geqslant 0, S_2 \geqslant 0, I_1 \geqslant 0, I_2 \geqslant 0, M \geqslant 0\},$$

$$X_0 = \{(S_1, S_2, I_1, I_2, B)|S_1 \geqslant 0, S_2 > 0, I_1 > 0, I_2 > 0, M > 0\},$$

$$\partial X_0 = X \setminus X_0.$$

Then X is the positive invariant set of X_0, and X_0 is relatively closed in X. Since the attracting domain $\Gamma = \{(S_1, S_2, I_1, I_2, B) \in R_+^5 : 0 < S_1 + S_2 + I_1 + I_2 \leqslant 1, 0 < B \leqslant \frac{p}{q}\}$ is a positive invariant set, system (4.16) is point dissipative. Define

$$M_\partial = \{(S_1(0), S_2(0), I_1(0), I_2(0), B(0))|S_1(t), S_2(t), I_1(t), I_2(t), B(t)$$
$$satisfy \quad system \ (4.16), (S_1(t), S_2(t), I_1(t), I_2(t), B(t)) \in \partial X_0, \forall \geqslant 0\}.$$

Let's prove $M_\partial = \{(S_1, 0, 0, 0, 0)|S_1 \geqslant 0\}$.

Supposing $\varphi_0 = (S_1(0), S_2(0), I_1(0), I_2(0), B(0)) \in M_\partial$ and there is $t_0 \geqslant 0$, such that at least one of the terms in $S_2(t), I_1(t), I_2(t), B(t)$ is greater than 0 at $t = t_0$. If $I_1(t_0) > 0, S_2(t_0) = I_2(t_0) = B(t_0) = 0$, then $B'(t_0) = \rho I_1(t_0) > 0$, that is to say that there is $t_1 > 0$, such that $I_1(t) > 0, B(t) > 0$ when $t_0 < t < t_0 + t_1$. So $(S_1(t), S_2(t), I_1(t), I_2(t), B(t)) \notin \partial X_0$, which contradicts $\varphi_0 \in M_\partial$. The same can be proved in other cases, so $M_\partial = \{(S_1, 0, 0, 0, 0)|S_1 \geqslant 0\}$. If the initial value $\psi_0 \in M_\partial, \cup_{\psi_0 \in M_\partial}\omega(\psi_0) = E_0$ since there is only one equilibrium E_0 in M_∂. Thus, E_0 is the compact isolated invariant set of M_∂ over the initial value ψ_0.

Then we will prove that there is a positive constant δ_0 ($0 < \delta_0 < \frac{1}{2}\frac{\mu+\gamma}{\beta+\alpha}(R_{0f}-1)$), such that for any solution $u(t,x_0), x_0 \in X_0$, $\limsup_{t\to\infty}\|u(t,x_0)-E_0\| \geqslant \delta_0$, that is, $W^S(E_0) \cap X_0 = \emptyset$, where $W^S(E_0)$ is the stable manifold of E_0. Let's prove it by proof by contradiction. Let's say for any $\delta_0 > 0$, we have $\limsup_{t\to\infty}\|u(t,x_0)-E_0\| < \delta_0$, i.e., there is a positive constant η_0, for any $t > \eta_0$, such that

$$1 - \delta_0 \leqslant S_1(t) \leqslant 1 + \delta_0, 0 \leqslant S_2(t), I_1(t), I_2(t), B(t) \leqslant \delta_0.$$

So, when $t > \eta_0$, we have

$$\frac{dI_1}{dt} > \beta(1-\delta_0)I_1 - \gamma I_1 - \mu I_1 - \alpha\delta_0 I_1 > \frac{1}{2}(\mu+\gamma)(R_{0f}-1)I_1,$$

then $\lim_{t\to\infty}I_1(t) = \infty$, which contradicts the hypothesis. Thus, E_0 is an isolated invariant set in set X, and $W^S(E_0) \cap X_0 = \emptyset$.

In conclusion, each of the forward orbital in M_∂ converges to E_0, and E_0 is aperiodic in M_∂. By the persistence theorem in Hale and Waltman (1989), system (4.16) is uniformly persistent when $R_{0f} > 1$. That completes the proof. □

Appendix B. The proof of the equivalence of M_s and M_f and the correlation between information transmission parameters and M_f

Now let's look for the relationship between M_s (3.10) and M_f (4.17). We can get $M_s > 0$ if and only if

$$h > (2 - \sigma_I - \sigma_S)\frac{\alpha\rho\beta}{q\gamma} + \frac{\beta^2}{\gamma} \doteq h_s. \tag{B.1}$$

and $M_f > 0$ if and only if

$$h > \frac{\beta^2}{\gamma\mu} + \frac{\rho}{d}\frac{\beta}{\gamma}\frac{\alpha}{(\mu+q)(\beta+q)} \\ \times [(2-\sigma_I-\sigma_S)q + (1-\sigma_I)\mu + (1-\sigma_I\sigma_S)\beta]. \tag{B.2}$$

Applying the parameter transformation (3.2) on (B.2), similarly, the parameters of subsequent models are still recorded as the original parameters, we have

$$h > \frac{\beta^2}{\gamma} + \frac{\alpha\rho\beta}{q\gamma}\frac{q}{\varepsilon\beta + q} \\ \times \frac{(2-\sigma_I-\sigma_S)q + (1-\sigma_I)\varepsilon + (1-\sigma_I\sigma_S)\beta\varepsilon}{\beta\varepsilon + q} \doteq h_f, \tag{B.3}$$

where $\varepsilon = \frac{\mu}{d}$. Then we have $h_f \to h_s$ as $\varepsilon \to 0$, which means that the condition for branching in the slow system (3.9) and the full system (4.16) are also equivalent on the basis of the huge variation in time between information dissemination and epidemiological and demographic process.

Recalling

$$M_f = \left(h\gamma - \frac{\beta^2}{\mu}\right)\frac{d}{\rho}(\mu+q)(\beta+q) \\ - [(2-\sigma_I-\sigma_S)q + (1-\sigma_I)\mu + (1-\sigma_I\sigma_S)\beta]\alpha\beta,$$

it is easy to testify that

$$\frac{\partial M_f}{\partial\sigma_S} > 0, \quad \frac{\partial M_f}{\partial\sigma_I} > 0, \quad \frac{\partial M_f}{\partial\alpha} < 0.$$

When $M_f > 0, h\gamma > \frac{\beta^2}{\mu}$ and $\left(h\gamma - \frac{\beta^2}{\mu}\right)\frac{d}{\rho} > \alpha\beta\frac{(2-\sigma_S-\sigma_I)q+(1-\sigma_I)\mu+(1-\sigma_I\sigma_S)\beta}{(\mu+q)(\beta+q)}$ must hold. So

$$\frac{\partial M_f}{\partial\rho} = -(\mu+q)(\beta+q)\left(h\gamma - \frac{\beta^2}{\mu}\right)\frac{1}{\rho^2} < 0,$$

and

$$\frac{\partial M_f}{\partial q} = \frac{d}{\rho}\left(h\gamma - \frac{\beta^2}{\mu}\right)(\mu+\beta+2q) - \alpha\beta(1-\sigma_I\sigma_S)$$

$$> \alpha\beta\frac{(2-\sigma_S-\sigma_I)q + (1-\sigma_I)\mu + (1-\sigma_I\sigma_S)\beta}{(\mu+q)(\beta+q)}(\mu+\beta+2q)$$

$$- \alpha\beta(2-\sigma_I-\sigma_S)$$

$$= \alpha\beta(2-\sigma_I-\sigma_S)\frac{q^2-\mu\beta}{(\mu+q)(\beta+q)} + \alpha\beta(1-\sigma_I)\frac{\mu(\mu+\beta+2q)}{(\mu+q)(\beta+q)}$$

$$+ \alpha\beta\frac{(1-\sigma_I\sigma_S)\beta}{(\mu+q)(\beta+q)}(\mu+\beta+2q)$$

$$> \alpha\beta(1-\sigma_I)\frac{\mu(\alpha+3q)}{(\mu+q)(\beta+q)} + \alpha\beta(1-\sigma_S)\frac{q^2-\mu\beta}{(\mu+q)(\beta+q)}$$

$$+ \alpha\beta(1-\sigma_I\sigma_S)\frac{\beta(\mu+\beta+2q)}{(\mu+q)(\beta+q)}$$

$$> \alpha\beta(1-\sigma_I)\frac{\mu(\alpha+3q)}{(\mu+q)(\beta+q)} + \alpha\beta(1-\sigma_S)\frac{q^2+\beta^2+2\beta q}{(\mu+q)(\beta+q)} > 0.$$

Appendix C. A model considering the infection induced by the asymptomatic infected individuals

Note that directly fitting the proposed model to data may induce a bias since our model does not consider the infection induced by the asymptomatic infected individuals, which were proven to be extremely important for epidemiology of COVID-19 (Amaral et al., 2021; Castro et al., 2020). We then simply extend our model by including a compartment of asymptomatic infected individuals. The corresponding equations are

$$\begin{cases} \frac{dS_1}{dt} = \mu - \beta S_1(I_1+\sigma_I I_2) - \psi\beta S_1(A_1+\sigma_A A_2) - \mu S_1 - \alpha BS_1 + qS_2 \\ \frac{dS_2}{dt} = -\beta\sigma_S S_2(I_1+\sigma_I I_2) - \psi\beta\sigma_S S_2(A_1+\sigma_A A_2) - \mu S_2 + \alpha BS_1 - qS_2 \\ \frac{dI_1}{dt} = k[\beta S_1(I_1+\sigma_I I_2) + \psi\beta S_1(A_1+\sigma_A A_2)] - \frac{\gamma_I I_1}{1+hI_1} - \mu I_1 - \alpha BI_1 + qI_2 \\ \frac{dI_2}{dt} = k[\beta\sigma_S S_2(I_1+\sigma_I I_2) + \psi\beta\sigma_S S_2(A_1+\sigma_A A_2)] - \frac{\gamma_I I_2}{1+hI_2} - \mu I_2 + \alpha BI_1 - qI_2 \\ \frac{dA_1}{dt} = (1-k)[\beta S_1(I_1+\sigma_I I_2) + \psi\beta S_1(A_1+\sigma_A A_2)] - \gamma_A A_1 - \mu A_1 - \alpha BA_1 + qA_2 \\ \frac{dA_2}{dt} = (1-k)[\beta\sigma_S S_2(I_1+\sigma_I I_2) + \psi\beta\sigma_S S_2(A_1+\sigma_A A_2)] - \gamma_A A_2 - \mu A_2 + \alpha BA_1 - qA_2 \\ \frac{dR_1}{dt} = \frac{\gamma_I I_1}{1+hI_1} + \gamma_A A_1 - \mu R_1 - \alpha BR_1 + qR_2 \\ \frac{dR_2}{dt} = \frac{\gamma_I I_2}{1+hI_2} + \gamma_A A_2 - \mu R_2 + \alpha BR_1 - qR_2 \\ \frac{dB}{dt} = \rho(I_1+\theta I_2) - dB \end{cases} \tag{C.1}$$

where k is the ratio of symptomatic infection, ψ is the relative transmission probability of A_1 compared with I_1, parameters σ_A ($0 < \sigma_A < 1$) represent the reduction factors in transmission rate when infection occurs between disease-unaware group S_1 and disease-aware group A_2, and γ_I and γ_A are recovery rates of symptomatic and asymptomatic infected individuals respectively.

We can testify that the feasible region of model (C.1) is

$$\Gamma = \Big\{ (S_1, S_2, I_1, I_2, A_1, A_2, R_1, R_2, B) \in R^{9+} : 0 < S_1, S_2, I_1, I_2, A_1, A_2, R_1, R_2 \leqslant S_1 \\ + S_2 + I_1 + I_2 + A_1 + A_2 + R_1 + R_2 \leqslant 1, 0 < B \leqslant \frac{\rho}{d} \Big\}.$$

which is a positively invariant set. A disease-free equilibrium $E_0 = (1,0,0,0,0,0,0,0,0)$ is always feasible. By calculating the spectral radius of the next generation for model (C.1), we get the basic reproduction number of this model is

$$R_0 = k\frac{\beta}{\gamma_I} + (1-k)\frac{\psi\beta}{\gamma_A}. \tag{C.2}$$

In the initial stage of the epidemic, we still assume that the total population is Wuhan residents, the conscious susceptible population is the isolated susceptible population, the conscious infected

population is the reported confirmed population and no individual was recovered. We also assume $\mu = 0$ because of the short epidemic time scale in comparison to the demographic time scale. We used the Least Square Method to fit the parameters in model (C.1) to study the effects of information transmission about disease caused by media coverage on COVID-19 infection as well. Data fitting gives the similar parameter estimations and a slightly great basic reproduction number as 3.30. This indicates that ignoring asymptomatic individuals may underestimate the COVID-19 infection. We mention here that the inclusion of asymptomatic individuals leads to a higher dimensional system, which is difficult to analyze theoretically, and we leave this for further study.

References

Amaral, M.A., Oliveira, M., Javarone, M.A., 2021. An epidemiological model with voluntary quarantine strategies governed by evolutionary game dynamics. Chaos Solitons and Fractals 143.

Andronov, A.A., Leontovich, E.A., Gordon, I.I., Maier, A.G., Gutzwiller, M.C., 1973. Qualitative theory of second-order dynamic systems. Phys. Today 27, 53–54.

Broer, H., 1995. Book review: Normal forms and bifurcations of planar vector fields. Bull. Am. Math. Soc. 32, 452–456.

Castillo-Chavez, C., Song, B., 2004. Dynamical models of tuberculosis and their applications. Math. Biosci. Eng. Mbe 1, 361.

Castro, M., Ares, S., Cuesta, J.A., Manrubia, S., 2020. The turning point and end of an expanding epidemic cannot be precisely forecast. Proc. Nat. Acad. Sci. 117, 26190–26196.

Cen, X., Feng, Z., Zhao, Y., 2014. Emerging disease dynamics in a model coupling within-host and between-host systems. J. Theor. Biol. 361, 141–151.

Cohen, J., Normile, D., 2020. New sars-like virus in china triggers alarm. Science 367, 234–235.

COV, 2020. Covid-19, unemployment, and suicide. Lancet Psychiatry 7, 389–390.

Crossley, T.F., Benzeval, M., Burton, J., Fisher, P., JöCkle, A., Read, B., Low, H., 2020. Briefing note covid-19 survey. In: Econ. Effects. Understanding Society Working Paper Series.

Cui, J., Mu, X., Hui, W., 2008a. Saturation recovery leads to multiple endemic equilibria and backward bifurcation. J. Theor. Biol. 254, 275–283.

Cui, J., Sun, Y., Zhu, H., 2008b. The impact of media on the control of infectious diseases. J. Dyn. Diff. Equat. 20, 31–53.

Dreessche, P., Watmough, J., 2002. Reproduction numbers and sub-threshold endemic equilibria for compartmental models of disease transmission. Math. Biol. 180, 29–48.

Feng, Z., Velasco-Hernandez, J., Tapia-Santos, B., 2013. A mathematical model for coupling within-host and between-host dynamics in an environmentally-driven infectious disease. Math. Biosci. 241, 49–55.

Feng, Z., Cen, X., Zhao, Y., Velasco-Hernandez, J.X., 2015. Coupled within-host and between-host dynamics and evolution of virulence. Math. Biosci. 270, 204–212.

Fenichel, N., 1979. Geometric singular perturbation theory for ordinary differential equations. J. Differ. Equ. 31, 53–98. https://doi.org/10.1016/0022-0396(79) 90152-9. http://www.sciencedirect.com/science/article/pii/ 0022039679901529.

Frank, N.T., 2020. Conditions for a second wave of covid-19 due to interactions between disease dynamics and social processes. Front. Phys. 8, 1–9.

Frederik, Verels, Lander, Wille, Philippe, Beutel, 2016. Behavioural change models for infectious disease transmission: a systematic review (2010–2015). J. R. Soc. Interface 13 (20160820), 2–20.

Funk, S., Gilad, E., Jansen, V.A.A., 2010a. Endemic disease, awareness, and local behavioral response. J. Theor. Biol. https://doi.org/10.1016/j.jtbi.2010.02.032.

Funk, S., Salathe, M., Jansen, V., 2010b. Modelling the influence of human behaviour on the spread of infectious diseases: a review. J. R. Soc. Interface 7, 1247–1256.

Gandolfi, A., Pugliese, A., Sinisgalli, C., 2015. Epidemic dynamics and host immune response: a nested approach. J. Math. Biol. 70, 399–435.

Hale, J.K., Waltman, P., 1989. Persistence in infinite-dimensional systems. In: Society for Industrial and Applied Mathematics.

Imai, N., Cori, A., Dorigatti, I., Baguelin, M., Donnelly, C., Riley, S., and Ferguson, N., 2020. Report 3: Transmissibility of 2019-ncov. https://www.imperial.ac.uk/ mrc-global-infectious-disease-analysis/covid-19/report-3-transmissibility-of-covid-19/. .

Jansen, V., Stollenwerk, N., Jensen, H.J., Ramsay, M.E., Edmunds, W.J., Rhodes, C.J., 2003. Measles outbreaks in a population with declining vaccine uptake. Science 301, 804.

Jinliang, W., Shengqiang, L., Baowen, Z., Yasuhiro, 2012. Qualitative and bifurcation analysis using an sir model with a saturated treatment function. Math. Comput. Model. 55, 710–722.

Khardori, N.M., 2009. Emergence of a novel swine-origin influenza a (h1n1) virus in humans. Yearbook of Medicine. https://doi.org/10.1016/s0084-3873(09)79323-x.

Li, Q., Guan, X., Wu, P., Wang, X., Zhou, L., Tong, Y., Ren, R., Leung, K., Lau, E., Wong, J., 2020. Early transmission dynamics in wuhan, china, of novel coronavirus–infected pneumonia. N. Engl. J. Med. 382.

National health commission of the people's republic of china. http://www.nhc.gov. cn/xcs/yqtb/202002/6c305f6d70f545d59548ba17d79b8229.shtml., 2020. .

Pcja, B., Pma, B., Pctb, A., 2021. Prioritising covid-19 vaccination in changing social and epidemiological landscapes: a mathematical modelling study. Lancet. Infect. Dis. https://doi.org/10.1016/S1473-3099(21)00057-8.

Reluga, T.C., Bergstrom, C.T., 2010. Game theory of social distancing in response to an epidemic. PLOS Comput. Biol. 6.

Samanta, S., Chattopadhyay, J., 2014. Effect of awareness program in disease outbreak – a slow-fast dynamics. Appl. Math. Comput. 237, 98–109.

Samanta, S., Rana, S., Sharma, A., Misra, A.K., Chattopadhyay, J., 2013. Effect of awareness programs by media on the epidemic outbreaks: A mathematical model. Appl. Math. Comput. 219, 6965–6977.

Schaller, M., 2011. The behavioural immune system and the psychology of human sociality. Philos. Trans. R. Soc. Lond. 366, 3418–3426.

Shannon, C., Kamran, K., Heffernan, J.M., Bauch, C.T., 2015. The effects of media reports on disease spread and important public health measurements. Plos One 10, e0141423.

Shim, D., 1991. Differential equations and dynamical systems. Springer-Verlag.

Smith, R.D., 2006. Responding to global infectious disease outbreaks: Lessons from sars on the role of risk perception, communication and management. Soc. Sci. Med. 63, 3113–3123.

Song, P., Xiao, Y., 2017. Global hopf bifurcation of a delayed equation describing the lag effect of media impact on the spread of infectious disease. J. Math. Biol. https://doi.org/10.1007/s00285-017-1173-y.

Song, P., Lou, Y., Xiao, Y., 2019. A spatial seirs reaction-diffusion model in heterogeneous environment. J. Differ. Equ. 267, 5084–5114.

Tang, B., Wang, X., Li, Q., Bragazzi, N.L., Tang, S., Xiao, Y., Wu, J., 2020. Estimation of the transmission risk of the 2019-ncov and its implication for public health interventions. Journal of. Clin. Med. 9.

Thompson, W.W., Shay, D.K., Weintraub, E., Cox, N., Anderson, L.J., Fukuda, K., 2003. Mortality associated with influenza and respiratory syncytial virus in the united states. JAMA J. Am. Med. Assoc. 289, 179–186.

Wang, A., Xiao, Y., 2014. A filippov system describing media effects on the spread of infectious diseases. Nonlinear Anal. Hybrid Syst. 11, 84–97.

Winskill, P., Whittaker, C., Walker, P.G., Watson, O. and Laydon, D., 2020. Report 22: Equity in response to the covid-19 pandemic: an assessment of the direct and indirect impacts on disadvantaged and vulnerable populations in low- and lower middle-income countries. https://www.imperial.ac.uk/mrc-global-infectious-disease-analysis/covid-19/report-22-equity/. .

Wise, T., Zbozinek, T.D., Michelini, G., Hagan, C.C., and Mobbs, D., 2020. Changes in risk perception and self-reported protective behaviour during the first week of the covid-19 pandemic in the united states. R. Soc. Open Sci., 7..

Xiao, Y., Zhao, T., Tang, S., 2013. Dynamics of an infectious diseases with media/ psychology induced non-smooth incidence. Math. Biosci. Eng. 10, 445–461.

Xiao, Y., Tang, S., Wu, J., 2015. Media impact switching surface during an infectious disease outbreak. Sci. Rep. 5, 7838.

Xu, R., Liu, X., 2008. Backward bifurcation of an epidemic model with saturated treatment function. J. Math. Anal. Appl. 348, 433–443.

Yan, Q., Tang, S., Gabriele, S., Wu, J., 2016. Media coverage and hospital notifications: Correlation analysis and optimal media impact duration to manage a pandemic. J. Theor. Biol. 390, 1–13.

Ying, L., Gayle, A.A., Annelies, W.S., Joacim, R., 2020. The reproductive number of covid-19 is higher compared to sars coronavirus. J. Travel Med. https://doi.org/ 10.1093/jtm/taaa021.

Zhang, S.X., Jiang, L.J., Zhang, Q.W., Pan, J.J., Wang, W.Y., 2004. Role of mass media during the severe acute respiratory syndrome epidemic. Chin. J. Epidemiol. 25, 403.

Zhao, S., Stone, L., Gao, D., Musa, S.S., Wa Ng, M.H., 2020. Imitation dynamics in the mitigation of the novel coronavirus disease (covid-19) outbreak in wuhan, china from 2019 to 2020. Ann. Transl. Med. 10.21037/atm.2020.03.168.

Zhou, X., Cui, J., 2011. Analysis of stability and bifurcation for an seir epidemic model with saturated recovery rate. Commun. Nonlinear Sci. Numer. Simul. 16, 4438–4450.

Zhou, W., Xiao, Y., Heffernan, J.M., Castro-Sānchez, E., 2019. Optimal media reporting intensity on mitigating spread of an emerging infectious disease. PLoS ONE 14.

Zhou, W., Wang, A., Xia, F., Xiao, Y., Tang, S., 2020. Effects of media reporting on mitigating spread of covid-19 in the early phase of the outbreak. Math. Biosci. Eng. 17, 2693–2707.